Applied Innovative Research
Vol. 1, June 2019, pp. 128-134

Graphene quantum dots (GQDs) from organic acids

Mude Jaya Prakash Naik, Peetam Mandal, Jhuma Debbarma & Mitali Saha*
NIT Agartala, Department of Chemistry, Agartala 799 046, India

Received 19 March 2019; accepted 19 June 2019

An environmentally eco-friendly method of synthesis of graphene quantum dots (GQDs) was reported using pyrolysis of organic acids, viz., tartaric acid and ascorbic acid at 150-160 °C, which produce (GQDs) in the presence of NaOH. The heating time and effect of different pH on the formation of GQDs have been studied in detail to optimize the reaction conditions. The UV-visible absorption and normalized fluorescence spectra have been applied to analyze the optical and luminescent properties of GQDs. The particles size distribution of the GQDs obtained from different organic acids at different pH has been also determined. The microstructures and surface morphology have been studied by atomic force microscope (AFM).

Keywords: Tartaric acid, Ascorbic acid, Pyrolysis, DLS, FTIR, AFM, GQDs

1 Introduction

Due to the unique optical and electronic properties, water solubility, excellent biocompatibility, low toxicity, and robust chemical inertness[1–3], graphene quantum dots (GQDs) has emerged as new carbon-based nanomaterial for wide applications in many field[4–8]. The number of scientific publications[9] on GQDs increases exponentially since 2006, and such explosion of interests are primarily due to their several merits including simple synthesis, low cost, and excellent biocompatibility. More than half of these research findings were established upon their photo-luminescent properties. In fact, the colorful photoluminescence, high photo-stability, and low toxicity of GQDs enable them strong competitors and potential alternatives to those heavy metal-based semiconductors currently in use[10-16].

Currently, numerous top-down and bottom-up preparation methods are the focus of attention, but the top down approaches such as laser ablation[17], electrochemical synthesis[18], arc discharge[19] involve a non-selective exfoliation process, and therefore may require toxic reagents and special equipments. Similarly, the bottom-up methods need several steps, strong acids and post treatments with surface passivating agents in order to improve their water solubility and luminescence property. Besides, most of these methods are time consuming and include the optimization of the hydrothermal treatment, temperature control and object selection. Sometimes, their photo-luminescence intensity was too weak to be available for the naked eye, thereby limiting the bioimaging and other optical applications.

In continuation of our earlier work[20], we have used eco-friendly method of pyrolysis of two organic acids, viz., tartaric and ascorbic acids, at 150-160 °C, followed by addition of trace amount of NaOH. During the synthesis, reproducibility is critically important for the potentially technological applications of GQDs. Hence, the effect of different pH on the formation of GQDs in presence of NaOH was studied in detail. This method required the optimization of the heating time as well as the pH of the solutions because the effect of heating time generally influences the degree of pyrolysis and carbonization of the organic acids, which finally influences the fluorescence intensity associated with the produced GQDs. The UV-visible absorption and normalized fluorescence spectra were applied to analyze the optical and luminescent properties of GQDs. The particles size distribution of the GQDs obtained from these organic acids at different pH was also determined by dynamic light scattering. The surface morphology and microstructures were studied by atomic force microscope (AFM).

2 Materials and Methods

Tartaric acid, ascorbic acid and sodium hydroxide were purchased from E Merck. Double distilled water was used throughout the experiment. The absorption spectra of GQDs obtained in each case was characterized by UV–Vis spectrophotometer (Shimadzu

*Corresponding author (E-mail: mitalichem71@gmail.com)

1800). The steady-state photoluminescence spectra were measured using florescence spectrophotometer (Perkin Elmer LS 55). The particle size distribution analysis was carried out using dynamic light scattering (DLS: Nanotrac wave W3222). The nano-morphology of GQDs was studied by atomic force microscopy (AFM, multimodeV8).

2.1 Pyrolysis of tartaric acid to prepare graphene quantum dots

Weighed amount of tartaric acid was heated and melted at around 150-160 °C, which then converted the colorless transparent solution into deep orange color within 35-40 min. 1.5 M solution of NaOH was added drop wise in the melted dense solution of tartaric acid at room temperature, to prepare the solutions of different pH ranging from 8 to 12. The effect of different pH on the yield and size of the graphene quantum dots (GQDs) was studied in detail. The probable mechanism of formation of GQDs from tartaric acid has been shown in the Scheme 1.

2.2 Pyrolysis of ascorbic acid to prepare graphene quantum dots (GQDs)

In a similar way, weighed amount of ascorbic acid was heated at around 150-160 °C, which then converted the solution into deep orange color within 50 min. 1.5 M solution of NaOH was added drop wise in the melted dense solution of ascorbic acid at room temperature, to prepare the solutions of different pH ranging from 8 to 12. The effect of different pH on the yield and size of the (GQDs) was studied in detail. The probable mechanism of temperature which then converted the solution into deep orange color within 50 min. 1.5 M solution of NaOH was added drop wise in the melted dense solution of ascorbic acid at room temperature, to prepare the solutions of different pH ranging from 8 to 12. The effect of different pH on the yield and size of the graphene quantum dots (GQDs) was studied in detail. The probable mechanism of formation of GQDs from ascorbic acid has been shown in the Scheme 2.

3 Results and Discussion

The plausible mechanism of the formation of GQDs from the organic acids viz., tartaric acid and ascorbic acid was explained in the Scheme 1. The tartaric and ascorbic acids when heated at their melting temperature decomposes and the hydronium ion formed from the acid, acted as a catalyst in subsequent decomposition reaction stages. The significant path in mechanism was that the condensation and cyclo-addition followed by the formation of aromatization and aromatic clusters. During the pyrolysis, adjacent dehydrated tartaric or ascorbic acid molecules reacted with each other to form GQDs, and the functional groups, such as -OH, -CH2-, -COOH, etc, located at the edge of each GQDs act as a passivation layer at the surface. This layer facilitates the uniform grouping of the sp2 clusters in the GQD structure, and these clusters are more or less isolated within the sp3 matrix; such structural adjustments enhance the luminescence of the GQDs. The formation of GQDs was not observed when pure tartaric acid or ascorbic acid was used, which indicated that NaOH acted as a catalyst for the formation of GQDs in each case. Observed at 340 nm

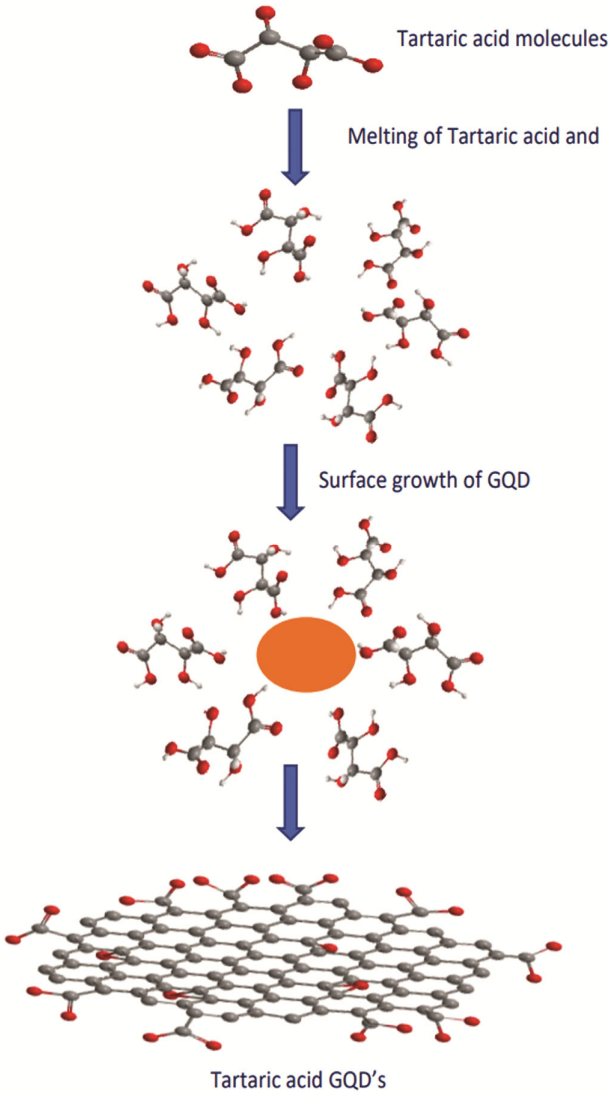

Scheme 1 — Probable mechanism of formation of GQDs from tartaric acid.

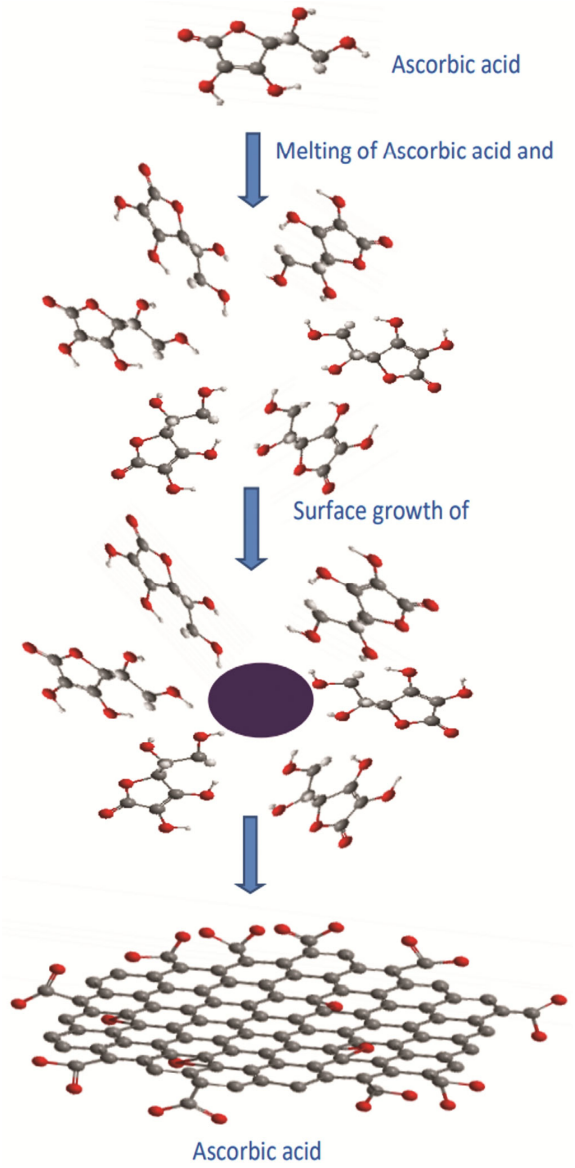

Scheme 2 — Probable mechanism of formation of GQDs from ascorbic acid.

(Fig. 1(b)). The UV-Vis spectra clearly indicated that on increasing the pH, the intensity of absorption peaks decreased. At pH 8, the absorption peak was found to be more intense and after this pH, the intensity of the peaks decreased up to 12. The GQDs prepared from tartaric acid typically showed two absorption maxima at 340 and 360 nm in case of entire pH range, with a tail extending to the visible range (Fig. 1 (a and b)). It can be attributed to the non-uniform size distribution of GQDs in presence of NaOH. The UV-Vis absorption may be attributed to some absorption shoulders for the π- π* transition of the C=C bonds, n-π* transition of C=O bonds and/or others. The spectra clearly indicated that on increasing the pH, the absorption peaks become broader which suggested the increase of distribution of particle size along with the pH. At pH 8, the absorption peak was found to be more intense but after this pH, the intensity of the peaks decreased up to 12. In case of ascorbic acid also, the UV-Vis spectra showed two absorption maxima at 310 and 340 nm at pH 8 and pH 9, which again can be attributed to the non-uniform size distribution of GQDs in presence of NaOH at these pH range. However, in case of pH 10-12, only one absorption maxima were observed at 340 nm (Fig. 1 (b)). The UV-Vis spectra clearly indicated that on increasing the pH, the intensity of absorption peaks decreased. At pH 8, the absorption peak was found to be more intense and after this pH, the intensity of the peaks decreased up to 12.

One of the most attractive features of GQDs, from application-focused on and ultimate perceptions, is their fluorescence. The prerequisite for surface passivation is only partly tacit but appears to be related to the synthetic method. However, more and more cases have arisen with λex independent emission position, which may be ascribed to their

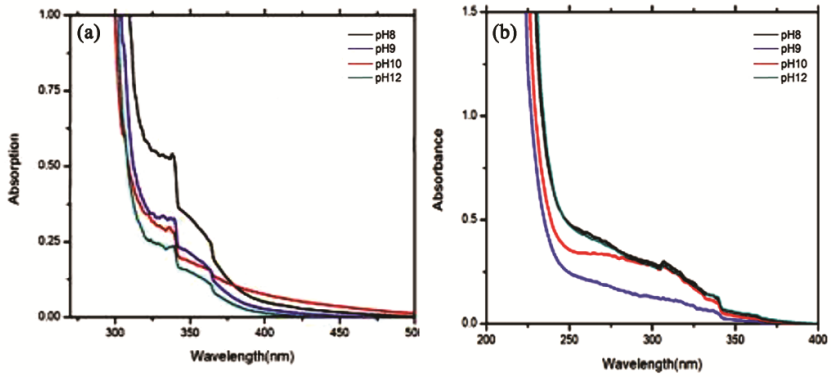

Fig. 1 — (a) UV-Visible spectra of GQDs prepared from tartaric acid at different pH and (b) UV-Visible spectra of GQDs prepared from ascorbic acid at different pH.

uniform size and surface chemistry. Our experimental results were displayed that the intensity of the fluorescence decreased with the increase of pH (Fig. 2). Captivatingly, in case of fluorescence also, the intensity of the peaks was found to be decreased from neutral to basic medium. The quantum yield of the GQDs was calculated using tryptophan as reported in previous literature[21]. The obtained quantum yield of ascorbic acid was found to be more than the tartaric acid, 2.5 % and 1.8 %, respectively.

The particle size distribution of the GQDs prepared from tartaric acid was carried out at 25 °C using dynamic light scattering (DLS). Figure 3 shows the particle size distribution of the solutions of different pH at room temperature. It was found that at pH 8, 90 % of particles were having the size around 1.3 nm. In case of pH 9, 80 % of the GQDs were found to be around 1.5 nm in size. On further increasing the pH from 10 to 12, the size of the particles drastically increased above 100 nm. The average particle size was found to be around 120 nm. It may be ascribed to the fact that in case of lower pH, the presence of hydroxyl groups mired the accumulation of the nanoparticles. On increasing the pH, the increasing number of hydroxyl groups may have got stick with the nanoparticles and hence resulted in the increase of the size. Thus, the pH of the solution of tartaric acid played an important role for the synthesis of GQDs with size below 5 nm.

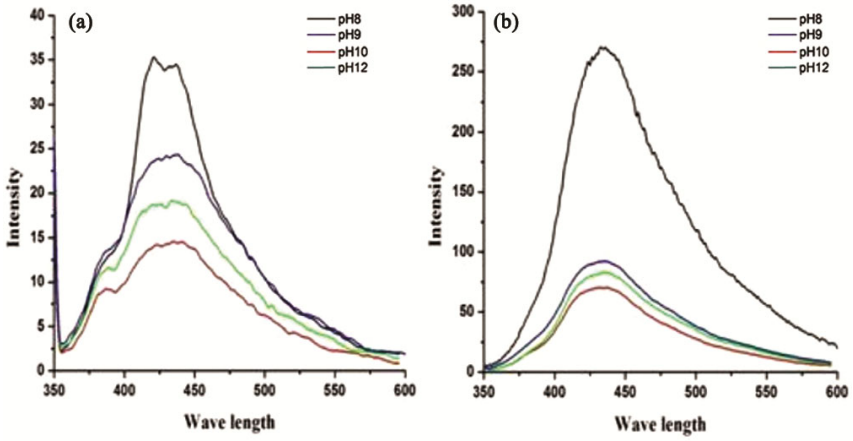

Fig. 2 — (a) Fluorescence curve of GQDs prepared from tartaric acid at different pH and (b) Fluorescence curve of GQDs prepared from ascorbic acid at different pH.

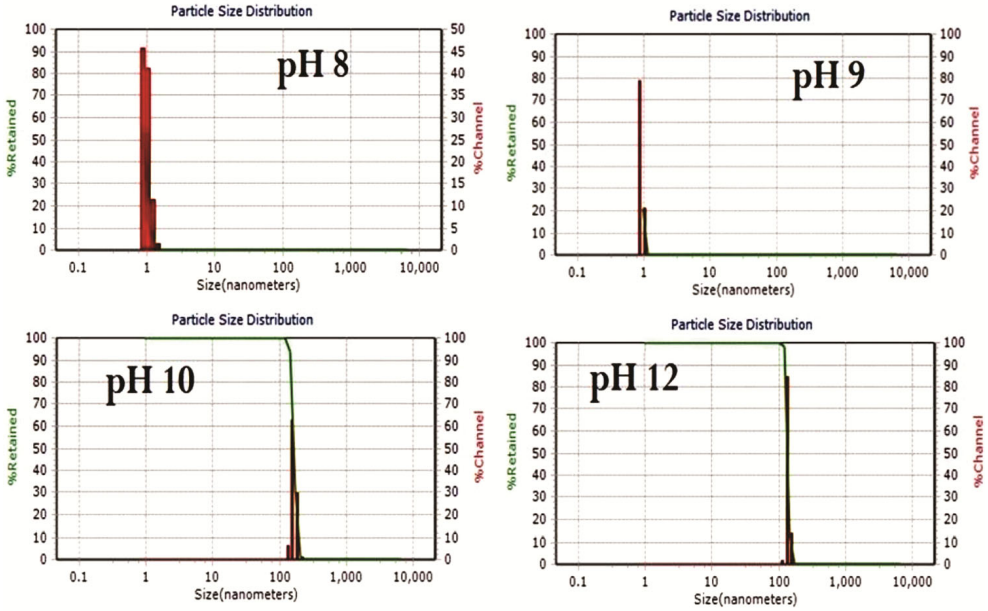

Fig. 3 — Particle size distribution curve of GQDs prepared from tartaric acid at different pH.

The particle size distribution of the GQDs prepared from ascorbic acid was carried out at 25 °C using dynamic light scattering (DLS). Figure 4 shows the particle size distribution of the solutions of different pH at room temperature. It was found that at pH 8, 60 % of the particles were found to be around 1 nm whereas in case of pH 9, 70 % of the GQDs were found to be around 1.5 nm in size. Here also, the size of the particles increased drastically, i.e., became more than 100 nm from pH 10 to 12. The average particle size was found to be around 500 nm. The same explanation was applicable here also that on increasing the pH, the increasing number of hydroxyl groups get adhered with the nanoparticles and hence resulted in the increase of the size of the nanoparticles.

The FTIR spectra of GQDs synthesized from tartaric acid exhibited several peaks related to the oxygen functional groups, viz., 3350 cm^{-1} (O-H stretching vibration), 1741 cm^{-1} (C=O stretching vibration) and 1620 cm^{-1} (aromatic C=C vibrations). The peak intensities were found to be weak which indicated that the hydroxyl and the carboxylic groups present in the tartaric acid condensed and polymerized to form GQDs (Fig. 5).

The FTIR spectra of GQDs from ascorbic acid showed the presence of different oxygen containing peaks at 3425 cm^{-1} (O-H stretching vibration), 1720 cm^{-1} (C=O stretching vibration) along with 1237 cm^{-1} (C-O-C bond) and 1615 cm^{-1} (aromatic C=C vibrations). The FTIR also confirmed that only hydroxyl and carboxyl groups were involved in the condensation and polymerization reactions but the C-O-C bonds were found intact as they were present in their precursor (Fig. 6).

The AFM showed the topographic images of well-dispersed GQDs prepared at pH 8 from tartaric acid (Fig. 7 (a and b)). It confirmed the formation of spherical shaped GQDs, where the particle sizes were below 5 nm at this pH. Figure 7 (c and d) showed the topographic images of well-dispersed GQDs prepared at pH 8 from ascorbic acid. Thus, it can be concluded that the pH of the solution played an important role for the formation of GQDs using organic acids, viz., tartaric and ascorbic acids in presence of NaOH.

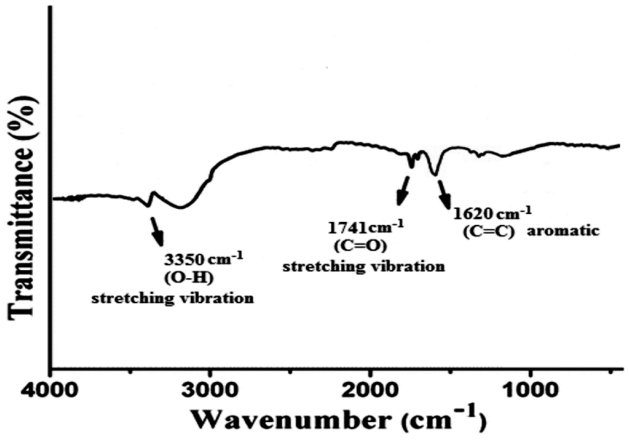

Fig. 5 — FTIR spectra of GQDs prepared from tartaric acid at pH 8

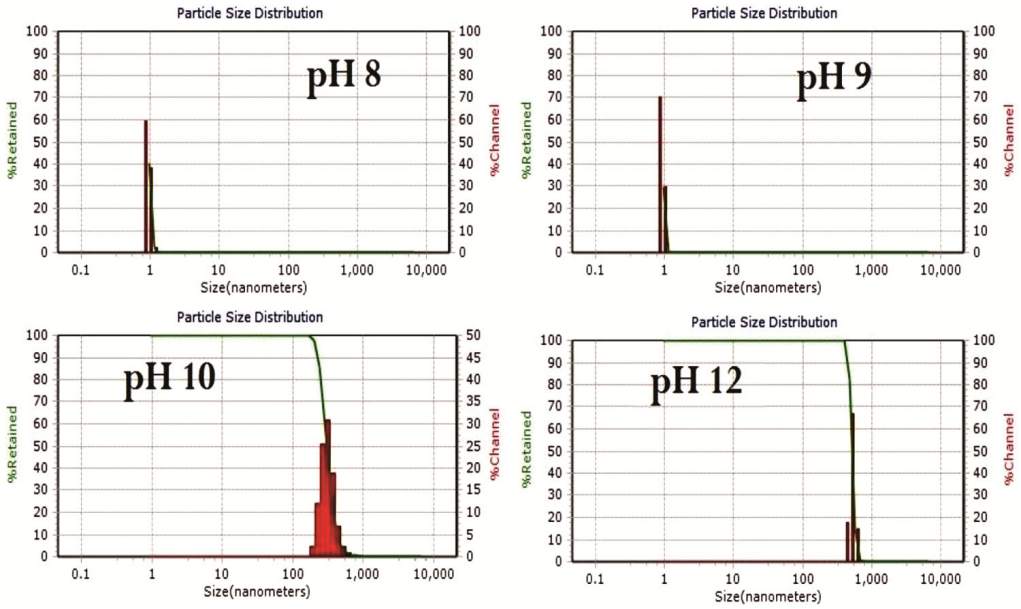

Fig. 4 — Particle size distribution curve of GQDs prepared from ascorbic acid at different pH.

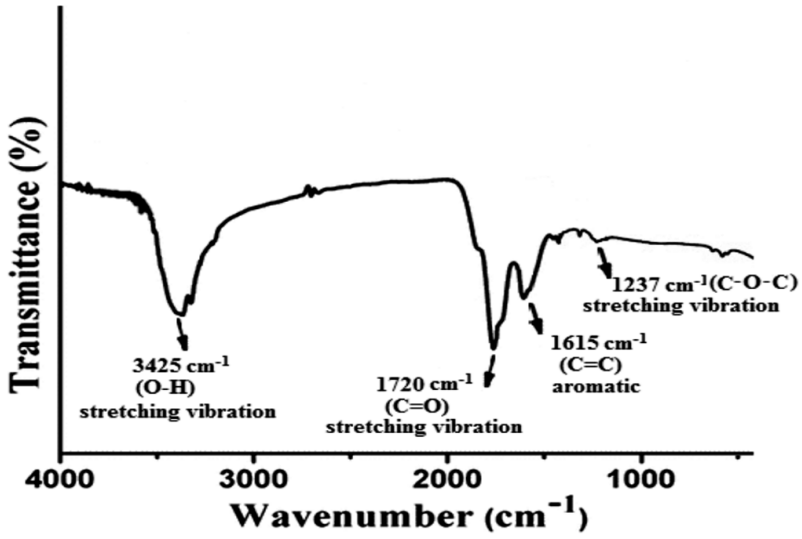

Fig. 6 — FTIR spectra of GQDs prepared from ascorbic acid at pH 8.

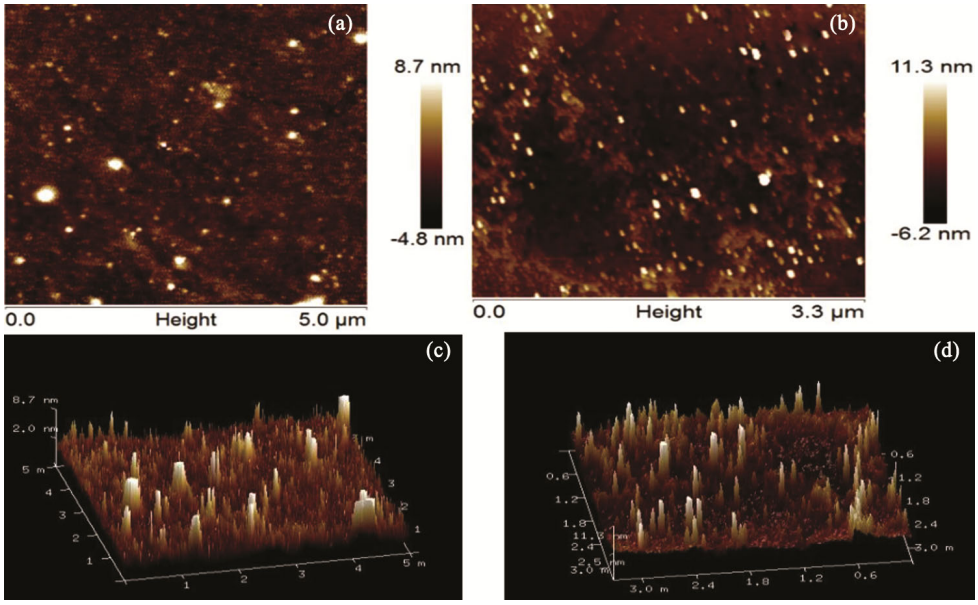

Fig. 7 — (a and b) AFM image of GQDs prepared from tartaric acid and ascorbic acid at pH 8; (c and d) AFM 3-D image of GQDs prepared from tartaric acid and ascorbic acid at pH 8.

4 Conclusions

In this paper, pyrolysis of tartaric acid and ascorbic acid was carried out at their melting temperatures, which decomposes and the hydronium ion formed from the acids, acted as catalyst in subsequent decomposition reaction stages. The formation of GQDs was not observed when pure tartaric acid or ascorbic acid was used, which indicated that NaOH acted as a catalyst for the formation of GQDs in each case. In case of tartaric acid, the UV-Vis spectra clearly indicated that on increasing the pH, the absorption peaks become broader, suggesting the increase of distribution of particle size along with the pH. Similar results were observed in case of ascorbic acid. The intensity of the fluorescence was also found to follow the same trend and decreased with the increase of pH. It was observed that at pH 8, 90 % of the particles have the size of around 1.3 nm in case of tartaric acid whereas in case of ascorbic acid, 70 % of the GQDs were found to be around 1.5 nm in size at pH 9. In both the organic acids, size

of the particles increased drastically, i.e., became more than 100 nm from pH 10 to 12. The AFM images confirmed the formation of spherical shaped GQDs. Thus, the pH plays a vital role for the formation of GQDs from tartaric acid and ascorbic acid in the presence of different organic acids. Further, it is also possible to control the formation of the GQDs by careful selection of carbon source and base.

Acknowledgement

Authors are grateful to Department of Chemistry for UV-Vis, fluorescence spectroscopy, DLS and FTIR studies and CRF, NIT Agartala for AFM characterizations.

References

1 Kanazawa H & Adachi S, *J Appl Phys*, 83 (1998) 5997.
2 Dantas N O, Paula P M N D, Silva R S, López-Richard V & Marques G E, *J Appl Phys*, 109 (2011) 024308.
3 Greben M, Fucikova A & Valenta J, *J Appl Phys*, 117 (2015) 144306.
4 Ullrich B, Xi H & Wang J S, *J Appl Phys*, 115 (2014) 233503.
5 Yousefi R, Mahmoudian M R, Sa´aedi A, Cheraghizade M, Jamali-Sheini F & Azarang M, *Ceram Int*, 42 (2016) 15209.
6 Al-Zuhery A M, Al-Jawad S M & Al-Mousoi A K, *Optik*, 130 (2017) 666.
7 Göde F & Ünlü S, *Mater Sci Semicond Process*, 90 (2019) 92.
8 Priyanka U, Akshay G K M, Elisha M G, Surya T B, Nitish N & Raj M B, *Int Biodeterior Biodegr*, 119 (2017) 78.
9 Soetedjo H, Siswanto B, Aziz I & Sudjatmoko, *Res Phys*, 8 (2018) 903.
10 Mamiyev Z Q & Balayeva N O, *Opt Mater*, 46 (2015) 522.
11 Nejo A O, Nejo A A, Pullabhotla R V S R & Revaprasadu N, *J Alloys Compd*, 537 (2012) 19.
12 Li M, Yang Y, Yuan X, Liu Y & Zhang L, *Mater Lett*, 149 (2015) 62.
13 Yücel E & Yücel Y, *Ceram Int*, 43 (2017) 407.
14 Joshi R K, Kanjilal A & Sehgal H K, *Appl Surf Sci*, 221 (2004) 43.
15 Onwudiwe D C, *Heliyon*, 5 (2019) e01413.
16 Davar F, Mohammadikish M, Loghman-Estarki M R & Masteri-Farahani M, *Ceram Int*, 40 (2014) 8143.
17 Yousefi R, Cheraghizade M, Jamali-Sheini F, Basirun W J & Huang N M, *Curr Appl Phys*, 14 (2014) 1031.
18 Beatriceveena T V, Prabhu E, Jayaraman V & Gnanasekar K I, *Mater Lett*, 238 (2019) 324.
19 Singh B P, Upadhyay R K, Kumar R, Yadav K & Areizaga-Martinez H I, *Adv Opt Technol*, 2016 (2016) 6.
20 Kaur N, Sharma S K, Kim D Y & Singh N, *Physica B: Condensed Matter*, 500 (2016) 179.
21 Sharma H K, Archana R, Sankarganesh R, Singh B P, Ponnusamy S, Hayakawa Y, Muthamizhchelvan C, Raji P, Kim D Y & Sharma S K, *Solid State Sci*, 94 (2019) 45.
22 Seetharaman A & Dhanuskodi S, *Spectrochim Acta Part A*, 127 (2014) 543.
23 Sharma S K, Baveja J & Mehra R M, *Physica Status Solidi A*, 194 (2002) 216.
24 Pentia E, Pintilie L, Matei I, Botila T & Pintilie I, *Inf Phys Technol*, 44 (2003) 207.